Elastic and thermal properties of mesotaxial $CoSi_2$ layers on Si

G. Bai, M-A. Nicolet, and T. Vreeland, Jr.
California Institute of Technology, Pasadena, California 91125

(Received 21 November 1990; accepted for publication 30 January 1991)

Single crystalline 110 nm thick $CoSi_2$ layers formed on both (100)- and (111)-oriented Si wafers by high dose ^{59}Co implantation and thermal annealing were analyzed by x-ray double crystal diffractometry. The lateral mismatch of both (100)- and (111)-oriented samples are similar ($\sim -0.7\%$) at room temperature, meaning that the average spacing between misfit dislocations is roughly the same (~ 30 nm). But the perpendicular mismatch differs for the two substrate orientations, reflecting the elastic anisotropy of the single-crystalline $CoSi_2$ layers. The three elastic constants of cubic $CoSi_2$ ($C_{11} = 277$, $C_{12} = 222$, $C_{44} = 100$ GPa) were extracted from these lattice mismatches and the sample curvature measurements. X-ray rocking curves were also recorded up to ~ 500 °C. The average spacing between the misfit dislocations remains unchanged, meaning that the misfit dislocations do not shear up to 500 °C. The linear thermal expansion coefficient of $CoSi_2$ (9.5×10^{-6}/°C) was obtained under the assumption that the elastic constants do not change with temperature.

I. INTRODUCTION

Following the successful growth of single crystalline $CoSi_2$ layers on Si(111) substrates by molecular beam epitaxy (MBE),[1] A. E. White and her colleagues demonstrated that such layers can also be formed by implantation of ^{59}Co into Si substrates and subsequent thermal annealing.[2] This "mesotaxy" technique has several advantages over the conventional vacuum deposition. The best mesotaxial layers have residual resistivity of $\sim 1\mu\Omega$ cm,[2] half of the value of the best MBE-grown films.[3] The layers grown on Si(111) by MBE deposition are B-type,[1] while the mesotaxial layers formed on Si(111) are mostly A-type.[4] The A-type mesotaxial layers enable one to make a high-precision determination of both lateral and perpendicular lattice mismatch by x-ray rocking curves. With B-type layers, the Bragg peaks from asymmetrical diffraction of the layers are widely separated from those of the substrates, precluding high-precision measurements of the lateral lattice mismatch.

Recognizing the opportunity that the mesotaxial A-type $CoSi_2$ layers on Si(111) offer, we measured both the perpendicular and parallel lattice mismatch in such layers, as well as those of mesotaxial layers formed on Si(100). These two measurements enable us to extract two ratios of the three independent elastic constants of cubic single crystal $CoSi_2$. We also measured the curvature of one sample to estimate the biaxial stress in the layer. These three measurements yield the absolute values of the three elastic constants of $CoSi_2$. We repeated similar measurements up to ~ 500 °C. Assuming that the elastic constants do not change between 20 °C and 500 °C, we are able to extract the linear thermal expansion coefficient for single crystal $CoSi_2$.

II. EXPERIMENTAL RESULTS AND DISCUSSION

A. Sample preparation

Single-crystalline buried $CoSi_2$ layers about 110 nm thick were formed by 200 keV $3 \times 10^{17}/cm^2$ ^{59}Co implantation at ~ 400 °C into Si substrates of both (100) and (111) orientation, followed by vacuum annealing at 600 °C for 60 min and 1000 °C for 30 min.[2] The top Si layers were then removed by reactive ion etching. Cross-sectional transmission electron microscopy shows that the interfaces between the layers and substrates are flat and atomically sharp.[2] MeV ^4He backscattering and channeling spectrometry indicate that the layers are stoichiometric and highly oriented, with a minimum yield of $\sim 3\%$.[2]

B. Lattice mismatch and misfit dislocations

Bulk $CoSi_2$ has a cubic CaF_2 structure, and a lattice mismatch with Si, $f = -1.22\%$, at room temperature. We used x-ray double crystal diffractometry to measure both the perpendicular and lateral lattice mismatch, $\epsilon^{\perp}$ and $\epsilon^{\parallel}$, between the $CoSi_2$ layer and the Si substrate. Figure 1 shows the Fe K_{α_1} (wavelength $\lambda = 0.1936$ nm) x-ray rocking curves from the symmetrical (400) and asymmetrical (311) diffraction planes of the $CoSi_2$/Si(100) sample. The two curves diffracted from the same (311) planes (A and B in Fig. 1) correspond to the x-ray incidence of opposite directions. The mismatch $\epsilon^{\perp}$ and $\epsilon^{\parallel}$ were extracted from the angular separations of the Bragg peaks between the layer and the substrate shown in Fig. 1. The results are listed in the first column of Table I. They are very close to those measured for buried $CoSi_2$ mesotaxial layers in the second column of Table I.[5] This agreement means that the Si capping layer has little effect on the strain state of the buried $CoSi_2$ layer. Unequal $\epsilon^{\perp}$ and $\epsilon^{\parallel}$ means that the $CoSi_2$ layer is distorted tetragonally under the tensile stress imposed by the Si substrate. The relative volume expansion, $\Delta V/V$, is $\sim 0.2\%$, more than three times less than the average linear dilatation, $\Delta L/L$, ($\sim 0.7\%$, see Table I).

The nonzero lateral mismatch means that there exist misfit dislocations at the interface to relax strain. The Burger's vector of the dislocations for epitaxial $CoSi_2$ layers on Si(100) substrates is $\mathbf{b} = 1/4\langle 111\rangle$.[6] The average

 0021-8979/91/096451-05$03.00

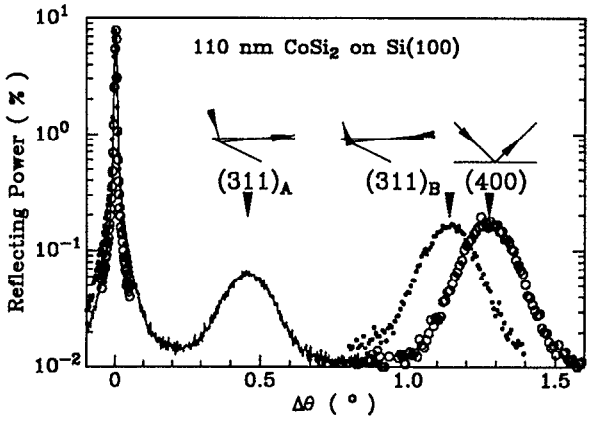

FIG. 1. Fe K_{α_1} x-ray ($\lambda = 0.1932$ nm) rocking curves of symmetrical (400) and asymmetrical (311) diffractions from $CoSi_2$/Si(100) sample. The diffraction geometry and direction of x-ray incidence are shown in the inset, marking the corresponded Bragg peaks from the $CoSi_2$ layer.

spacing, p, between the misfit dislocations is therefore

$$p = \frac{b_m}{|\epsilon^{\parallel}|} = \frac{0.19 \text{ nm}}{0.62\%} = 31 \text{ nm}, \tag{1}$$

where b_m is the edge component of Burger's vector projected onto the interface plane. This is roughly the same as that of MBE-grown thick (>10 nm) B-type $CoSi_2$/Si(111) samples (~ 30 nm).[1]

Single crystalline $CoSi_2$ has three independent elastic constants, C_{11}, C_{12}, C_{44}. Measurements of the lattice distortion of $CoSi_2$ layers on Si substrates of two different orientations enable one to extract two ratios, C_{12}/C_{11} and C_{44}/C_{11}. From the definition of the lattice mismatch and the elastic strain, $e^{\perp}$ and $e^{\parallel}$, one has the following relationship,

$$\frac{e^{\perp}}{e^{\parallel}} = \frac{\epsilon^{\perp} - f}{\epsilon^{\parallel} - f}. \tag{2}$$

Assuming that the layer is under biaxial stress in the (100) plane, the relation[7]

$$\frac{e^{\perp}}{e^{\parallel}} = -\frac{2C_{12}}{C_{11}}, \tag{3}$$

holds in the linear elasticity theory. From the measured lattice mismatch (Table I) and Eqs. (2) and (3), the ratio C_{12}/C_{11} is obtained (Table II). This value (0.80) is about

TABLE I. Lattice distortion of $CoSi_2$ layers on (100) and (111) oriented Si substrates. Data for Si/$CoSi_2$/Si samples are from Ref. 5 and that for B-type sample is from Ref. 8.

$f = -1.22\%$	$CoSi_2$/ Si(100)	Si/$CoSi_2$/ Si(100)	$CoSi_2$/ Si(111)	Si/$CoSi_2$/ Si(111)	B-$CoSi_2$/ Si(111)
$\epsilon^{\perp}$ (%)	−2.18	−2.14	−1.69	−1.74	−1.61
$\epsilon^{\parallel}$ (%)	−0.62	−0.66	−0.72	−0.66	−0.80
$\Delta L/L$ (%)	0.7	0.7	0.5	0.6	0.4
$\Delta V/V$ (%)	0.2	0.2	0.5	0.6	0.5

TABLE II. Ratios and elastic constants (in units of GPa) of cubic $CoSi_2$ from strain and curvature measurements. Data for Si is from Ref. 7 and listed for comparison.

	$\nu_{(100)}$	$\nu_{(111)}$	C_{12}/C_{11}	C_{44}/C_{11}	C_{11}	C_{12}	C_{44}
$CoSi_2$	0.44	0.32	0.80	0.36	277	222	100
Si	0.28	0.18	0.39	0.48	166	64	80

twice that of silicon (0.39).[7] For later convenience, we define the Possion ratio, ν, for thin films under biaxial stress, according to

$$\frac{e^{\perp}}{e^{\parallel}} = \frac{-2\nu}{1-\nu}. \tag{4}$$

This yields $\nu_{(100)} = 0.44$ for the $CoSi_2$ layer on Si(100) substrate (Table II).

Similarly, both symmetrical (111) and asymmetrical (311) x-ray rocking curves were also recorded for the $CoSi_2$/Si(111) sample. The perpendicular and parallel lattice mismatch were extracted from the Bragg peak separations. The results are given in Table I, which again agree well with those for buried $CoSi_2$ layers ($\epsilon^{\perp} = -1.74\%$ and $\epsilon^{\parallel} = -0.66\%$).[5] Furthermore, they are also about the same as those for MBE-deposited B-type $CoSi_2$ layers on Si(111) substrates ($\epsilon^{\perp} = -1.61\%$ and $\epsilon^{\parallel} = -0.80\%$).[8] This shows that the strain state of thick (>10 nm) epitaxial $CoSi_2$ layers on Si(111) substrates is independent of the process by which the silicide layers are formed, and whether the layers are type A or type B. The Burger's vector of the misfit dislocations is $\mathbf{b} = 1/6\langle 112\rangle$ for both type A $CoSi_2$ formed by ^{59}Co implantation[5] and type-B layer by MBE[1] on Si(111) substrates. The average misfit dislocation spacing is therefore $p = 31$ nm, obtained from Eq. (1) and Table I. This is the same as that on Si(100), implying that the dislocation spacing is independent of substrate orientation.

The areal density, ρ, of imperfections such as threading dislocations in epitaxial $CoSi_2$ layers can be estimated from the measured x-ray peak broadening, $(\delta\theta)$, using the equation[9]

$$\rho = \frac{(\delta\theta)^2 - (\delta\theta)_S^2}{9b^2}. \tag{5}$$

The size broadening, $(\delta\theta)_S$, is obtained from the Scherrer equation,

$$(\delta\theta)_S = \frac{0.94\lambda}{2t_l \cos\theta_B}, \tag{6}$$

where t_l is the layer thickness and θ_B the Bragg angle. The imperfection density estimated from Eq. (5) varies from $\sim 2 \times 10^9/\text{cm}^2$ for the (100) and (111) $CoSi_2$ layers formed by Co implantation (see the peak broadening in Fig. 1) to $< 10^7/\text{cm}^2$ for the best MBE-grown B-type $CoSi_2$ layer on Si(111) that we have measured.[8] However, the average misfit dislocation spacing is about the same (~ 30 nm) for all samples. This means that the strain relaxation and the imperfections in the layer are unrelated,

suggesting that the misfit dislocations nucleate at interfacial defects such as atomic steps rather than on the surface. We therefore speculate that specular Si surfaces free of any surface defects such as atomic steps are needed to grow metastable pseudormorphic $CoSi_2$ layers (>10 nm). The inference then is that high-dose ^{59}Co implantation will not produce metastable pseudormorphic $CoSi_2$ layers because defects like atomic steps are always present at the silicide/silicon interface in this case. This is unlike the relaxation of epitaxial GeSi layers on Si, where the strain relaxation necessarily yields to threading dislocations in the layer because misfit dislocations nucleate at the surface and glide down to the interface.[10]

In summary, all these observations suggest that the strain relaxation of thick (>10 nm) epitaxial $CoSi_2$ layers is intrinsic to the silicide, and insensitive to the type of the layer (A or B), the silicide formation process (high dose implantation or vacuum deposition), the orientation of the substrate, the imperfections in the layer, and the thickness of the layers.[8] This is in contrast with epitaxial GeSi layers grown on Si substrates, where the misfit dislocation spacing is very sensitive to the growth temperature and layer thickness for a fixed lattice mismatch.[11]

The perpendicular mismatch $\epsilon^{\perp}$ of the $CoSi_2$ layer is distinctly smaller on Si(111) than on Si(100) (Table I), showing that single-crystalline $CoSi_2$ layers are elastically anisotropic. This means that the bond strength between (111) planes is stronger than that between (100) planes. This result is similar to that of silicon where the covalent bond along the $\langle 111\rangle$ direction gives rise to the strongest bond between the (111) planes. On Si(111), the relative volume expansion of the $CoSi_2$ layer is $\sim 0.5\%$, the same as the average linear dilatation ($\sim 0.5\%$, Table I).

To extract the second ratio C_{14}/C_{11} from the measurements on the (111) sample, the procedure outlined for the (100) case was repeated with Eq. (2) and a suitably modified Eq. (3),[7]

$$\frac{e^{\perp}}{e^{\parallel}}=\frac{C_{44}-(C_{11}+2C_{12})/2}{C_{44}+(C_{11}+2C_{12})/4}. \tag{7}$$

The result is given in Table II. This ratio (0.36) is less than that of silicon (0.48).[7] The Possion ratio is $\nu_{(111)} = 0.32$, obtained from Eqs. (2) and (4) and Table I. It is the same as that for MBE-grown B-type $CoSi_2$ layers on Si(111) substrates ($\sim 1/3$).[8]

C. Stress and sample bending

To obtain the absolute values of the elastic constants, the biaxial tensile stress in the $CoSi_2$ layer, σ_l, was estimated by measuring the bending of the $CoSi_2$/Si(100) sample. The stress is related to the tensile strain in the plane according to Hooke's law in the linear elasticity,

$$\sigma_l=B_l\epsilon^{\parallel}=B_l(\epsilon^{\parallel}-f), \tag{8}$$

where B_l is the biaxial elastic constant of the layer. The stress causes the sample to bend with a concave radius of curvature, R. In the case where the thickness of the substrate, t_s, is much larger than that of the layer t_l and is smaller than the lateral dimension of the sample, the following relationship holds,[12]

$$\sigma_l=\frac{B_s t_s^2}{6Rt_l}, \tag{9}$$

where B_s is the biaxial elastic constant of the substrate. Combing Eqs. (8) and (9), one has

$$\frac{B_l}{B_s}=\frac{t_s^2}{6Rt_l}\frac{1}{\epsilon^{\parallel}-f}. \tag{10}$$

The radius R was obtained by measuring the angular difference of the (400) Bragg peaks diffracted from the substrate at two different spots of the sample separated by 4 mm, using a double crystal diffractometer equiped with a translational stage. Substituting appropriate parameters for the aforementioned $CoSi_2$/Si(100) sample, we obtain the ratio $B_l/B_s = 0.8$ from Eq. (10). Knowing $B_s = 180$ GPa for Si(100),[7] we obtain $B_l = 144$ GPa for $CoSi_2$(100). This value agrees well with that extracted from thermal stress measurement by van Ommen *et al.* (140 GPa).[13] It is slightly larger than the measured biaxial elastic constants of several transition-metal disilicide films (Ti, Ta, Mo, W) on Si(100) substrates (~ 110 GPa).[14] The biaxial elastic constant of (100) oriented films equals[7]

$$B=C_{11}\left[1+\frac{C_{12}}{C_{11}}-2\left(\frac{C_{12}}{C_{11}}\right)^2\right]. \tag{11}$$

From the the measured values of B and C_{12}/C_{11} for the $CoSi_2$(100) layer, the absolute value of C_{11} can be obtained from Eq. (11). We thus have all three elastic constants of single crystalline $CoSi_2$ (Table II). Lambrecht *et al.*[15] studied theoretically the electronic band structure of $CoSi_2$ using the linear muffin tin orbital method and calculated the bulk mudulus of $CoSi_2$ to be 190 GPa. In comparison, we used the elastic constants in Table II and obtained the bulk modulus of 240 GPa, about 25% larger than this theoretical estimate.

D. Dislocation locking and thermal stress

To extract the linear thermal expansion coefficient of $CoSi_2$ and study the thermal stress, we measured the lateral and perpendicular lattice mismatch between $CoSi_2$ layers and Si substrates up to 500 °C. The lattice mismatch f between stress-free $CoSi_2$ and Si equals

$$f=\left(\frac{1-\nu}{1+\nu}\right)\epsilon^{\perp}+\left(\frac{2\nu}{1+\nu}\right)\epsilon^{\parallel} \tag{12}$$

from Eqs. (2) and (4). Assuming that the Possion ratio ν does not change with temperature, f can then be extracted from the ν obtained at room temperature (Table II) and the measured $\epsilon^{\perp}$ and $\epsilon^{\parallel}$ at various temperatures (Fig. 2). f decreases linearly with rising temperature up to 500 °C (open and filled circles in Fig. 2). The slope yields the difference between the linear thermal expansion coefficients of $CoSi_2$ and Si. The slope has the same value, within the experimental error, for both the (100) and (111) samples [Figs. 2(a) and 2(b)], which averages $(6.5 \pm 0.6) \times 10^{-6}$/°C. This result shows that the thermal expansion

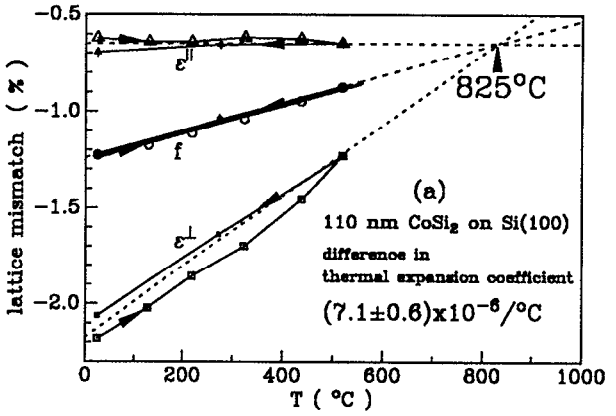

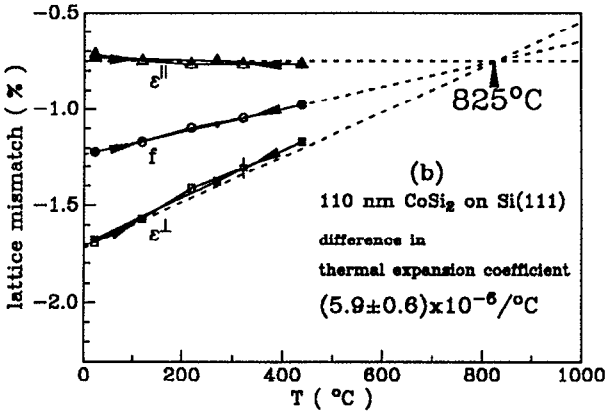

FIG. 2. The lattice mismatch, $\epsilon^{\perp}$ (square), $\epsilon^{\parallel}$ (triangle), and f (circle), as a function of the measurement temperature for both (a) the $CoSi_2$/Si(100) and (b) the $CoSi_2$/Si(111) samples. Open (filled) symbols are for the measurements when the temperature was raised (lowered).

coefficient of $CoSi_2$ is isotropic, in accord with the fact that the unit cell of stress-free $CoSi_2$ is cubic. The linear thermal expansion coefficient of bulk Si is known to be 3×10^{-6}/°C between 23 and 500 °C.[16] The coefficient for $CoSi_2$ layers is therefore 9.5×10^{-6}/°C, in good agreement with that reported for bulk $CoSi_2$ polycrystalline samples (9.4×10^{-6}/°C).[17] It is smaller than the linear thermal expansion coefficients of several transition-metal disilicides (Ti, Ta, Mo, W) ($\sim 15 \times 10^{-6}$/°C).[14]

The lateral mismatch $\epsilon^{\parallel}$ of $CoSi_2$ layers on both Si(100) and Si(111) substrates does not change up to 500 °C [open and filled triangles in Figs. 2(a) and 2(b)]. This means that the misfit dislocations do not shear up to 500 °C. By extrapolating $\epsilon^{\parallel}$ and $\epsilon^{\perp}$ to higher temperatures, we found that they meet (and consequently f also) at 825 °C, for both (100) and (111) samples [Figs. 2(a) and 2(b)]. This indicates that the $CoSi_2$ layer is fully relaxed at $\sim$800 °C.

E. Synthesis and model

Based on the above results, we propose the following model: (1) the strain in epitaxial $CoSi_2$ layers on Si substrates reaches the equilibrium value at a relaxation temperature T_R; (2) the misfit dislocations do not shear below

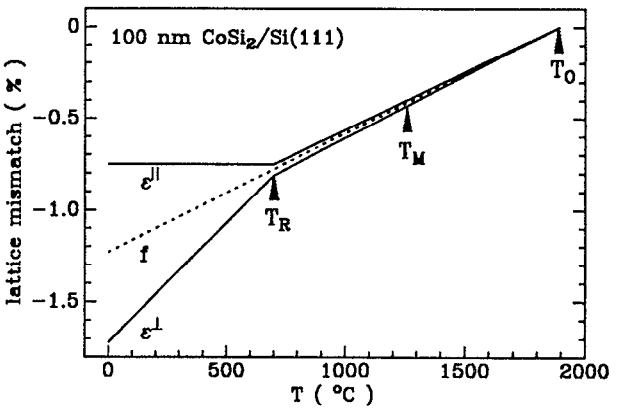

FIG. 3. Schematics of the proposed model showing how an epitaxial $CoSi_2$ layer relaxes to an equilibrium strain state at T_R and above, and that misfit dislocations are locked-in below T_R. T_M is the melting temperature of $CoSi_2$ and T_O is the hypothetical temperature at which the lattice mismatch between $CoSi_2$ and Si becomes zero.

T_R. According to Matthews and Blakeslee's strain relaxation model,[18] the equilibrium critical thickness, t_{cr}, for a pseudormorphic layer is[18]

$$t_{cr}=\frac{b}{8\pi(1+\nu)|f|}\left(\ln\frac{t_{cr}}{b}+1\right). \tag{13}$$

For a layer of thickness t_l larger than t_{cr}, the equilibrium lateral mismatch $\epsilon^{\parallel}_{eq}$ equals[18]

$$\epsilon^{\parallel}_{eq}=f\left(1-\frac{t_{cr}}{t_l}\frac{\ln t_l/b+1}{\ln t_{cr}/b+1}\right). \tag{14}$$

We apply these predictions to a 110 nm thick $CoSi_2$ layer on a Si(111) substrate. Assuming $T_R = 700$ °C, the lattice mismatch equals $f = -0.78\%$ at this relaxation temperature (Fig. 3). The equilibrium critical thickness is 3 nm from Eq. (13) ($\mathbf{b} = 1/6\langle 112\rangle$ and $\nu = 1/3$). This value agrees well with the measured critical thickness of B-type $CoSi_2$ grown on Si(111) by MBE at $\sim$650 °C ($\sim$3 nm).[19] For that same 110 nm thick $CoSi_2$ at $T_R = 700$ °C, the equilibrium lateral mismatch equals $\epsilon^{\parallel}_{eq} = 0.95f = -0.74\%$ from Eq. (14), and the perpendicular one equals $\epsilon^{\perp}_{eq} = -0.82\%$ from Eq. (12) (Fig. 3). Above T_R, misfit dislocations are generated by either nucleation or multiplication, or both, to minimize the strain energy so that the equilibrium state maintains (Fig. 3). Below T_R, the misfit dislocations are locked in and the lateral lattice mismatch $\epsilon^{\parallel}$ remains constant (Fig. 3). Thermal strain and stress are generated by the different thermal expansions between the layer and the substrate. At room temperature, the lateral mismatch $\epsilon^{\parallel}$ remains the same (-0.74%) and the perpendicular one $\epsilon^{\perp}$ decreases to -1.70% according to Eq. (12) (Fig. 3). These estimates agree well with experimental observations (Table I). The exact value of $\epsilon^{\parallel}$ at room temperature depends on the relaxation temperature T_R. An increase of T_R from 600 to 800 °C causes a corresponding increase of f from -0.84% to -0.71%. This change raises $\epsilon^{\parallel}$ from -0.80% to -0.67% according to Eq. (14). This shows that the lateral lattice mismatch is not

sensitive to the change in T_R and explains the observed apparent universal lateral mismatch at room temperature (Table I).

The relaxation temperature, T_R, depends on many factors such as the formation process of the silicides. It varies from ~ 600 °C for MBE-grown $CoSi_2$ on Si at ~ 600 °C to ~ 800 °C for the sample formed by high dose ^{59}Co implantation followed by 1000 °C vacuum annealing for 30 min. Figure 2(a) also shows that the thermal strain in the layer relaxes slightly after heating in ambient air at ~ 500 °C for ~ 2 h, even if the sample had been annealed in vacuum at 1000 °C for 30 min. This suggests that thermal annealing in ambient air lowers the relaxation temperature T_R. This phenomenon is similar to what we observed for MBE-grown B-type $CoSi_2$ layers on Si(111) substrates. There the thermal stress also relaxes slightly after thermal annealing in ambient air at ~ 600 °C for ~ 2 h,[8] but remains unchanged after vacuum annealing at ~ 800 °C for 1 h. Auger electron spectroscopy of the ambient-air annealed MBE-grown sample shows that a thin oxide of ~ 10 nm is present on the surface of the silicide that is absent in the vacuum annealed sample. An oxidation of the $CoSi_2$ at its surface induces atomic rearrangements at the silicide/silicon interface.[20] These observations indicate that atomic transport at the silicide/silicon interface lowers the relaxation temperature T_R (see also discussions in Ref. 8).

III. CONCLUSION

We obtained three elastic constants of cubic $CoSi_2$ by measuring the strain and stress in $CoSi_2$ layers on Si substrates at room temperature using double crystal x-ray diffractometry. X-ray rocking curves were also used to measure the lattice mismatch between the layer and substrate at elevated temperatures up to 500 °C. A linear thermal expansion coefficient of 9.5×10^{-6}/°C was derived for $CoSi_2$. The lateral mismatch at room temperature is about the same ($\sim -0.7\%$) for all the samples, regardless of the silicide formation process and the substrate orientation. It does not change with temperature up to 500 °C. The universal lateral mismatch was explained by the model that $CoSi_2$ layers reach an equilibrium strain state at a relaxation temperature T_R (~ 600–800 °C) by generation of misfit dislocations and the dislocations are locked-in below T_R. We proposed that atomic flux across the silicide/silicon interface lowers T_R. We also speculate that perfectly flat Si surfaces free of defects such as atomic steps are needed for the growth of metastable pseudormorphic $CoSi_2$ layers (> 10 nm).

ACKNOWLEDGMENTS

The authors thankfully acknowledge the collaboration of A. E. White in this project and the technical assistance of K. T. Short, at AT&T Bell Laboratories, where the samples originated, A. Venezia, at Rafael, for Auger measurements, and R. Gorris, at Caltech, for technical support. This paper is based upon work supported in part by the Semiconductor Research Corporation under contract No. 100-SJ-90 and by the National Science Foundation under grant No. DMR-8811795. The authors gratefully acknowledge this support.

[1] R. T. Tung, J. C. Bean, J. M. Gibson, J. M. Poate, and D. C. Jacobson, Appl. Phys. Lett. **40**, 684 (1982).
[2] A. E. White, K. T. Short, R. C. Dynes, J. P. Garno, and J. W. Gibson, Appl. Phys. Lett. **50**, 95 (1987).
[3] J. C. Hensel, R. T. Tung, J. M. Poate, and F. C. Unterwald, Appl. Phys. Lett. **44**, 913 (1984).
[4] C. W. T. Bulle-Lieuwma, A. H. van Ommen, and L. J. van IJzendoorn, Appl. Phys. Lett. **54**, 244 (1989).
[5] J. M. Vandenberg, A. E. White, R. Hull, K. T. Short, and S. M. Yalisove, J. Appl. Phys. **67**, 787 (1990).
[6] S. M. Yalisove, R. T. Tung, and D. Loretto, J. Vac. Sci. Technol. A **7**, 1472 (1989).
[7] W. A. Brantley, J. Appl. Phys. **44**, 534 (1973).
[8] G. Bai, M-A. Nicolet, T. Vreeland, Jr., Q. Ye, and K. L. Wang, Appl. Phys. Lett. **55**, 1874 (1989).
[9] P. Gay, P. B. Hirsch, and A. Kelly, Acta Metal. **1**, 315 (1953).
[10] R. Hull, J. C. Bean, D. J. Werder, and R. E. Leibenguth, Appl. Phys. Lett. **52**, 1605 (1988).
[11] J. C. Bean, L. C. Feldman, A. T. Fiory, S. Nakahara, and I. K. Robinson, J. Vac. Sci. Technol. A **2**, 436 (1984).
[12] R. F. S. Hearmon, *An Introduction to Applied Anisotropic Elasticity* (Oxford University, London, 1961), Ch. VII.
[13] A. H. van Ommen, C. W. T. Bulle-Lieuwma, and C. Langereis, J. Appl. Phys. **64**, 2706 (1988).
[14] T. F. Retajczyk, Jr. and A. K. Sinha, Thin Solid Films **70**, 241 (1980).
[15] W. R. L. Lambrecht, N. E. Christensen, and P. Blöchl, Phys. Rev. B **36**, 2493 (1987).
[16] H. F. Wolf, *Silicon Semiconductor Data* (Pergamon Press, New York, 1969) p. 101.
[17] M-A. Nicolet and S. S. Lau, in *VLSI Electronics*, Vol. 6, edited by N. G. Einspruch and G. B. Larrabee (Academic, New York, 1983), p. 330.
[18] J. W. Matthews and A. E. Blakeslee, J. Cryst. Growth **27**, 118 (1974).
[19] J. L. Batston, J. M. Gibson, and J. M. Poate, Mat. Res. Soc. Proc. **91**, 445 (1987).
[20] M. Bartur and M-A. Nicolet, Appl. Phys. A **29**, 69 (1982).